

Electro-optical sampling at near-zero optical bias

Yuelin Li^{a)}

Accelerator Systems Division, Argonne National Laboratory, 9700 South Cass Avenue, Argonne, Illinois 60439

(Received 14 February 2006; accepted 18 May 2006; published online 20 June 2006)

We report a detailed study of distortion effects in electro-optical sampling measurement at near-zero optical bias. It is found that when the induced optical retardation has a dynamic range larger than the optical bias, a false polarity change of the field can be observed merely due to the amplitude change of the field under investigation. The distortion cannot be corrected in general. However, when the optical bias is known, this phenomenon can be exploited to derive the absolute field amplitude under study. © 2006 American Institute of Physics. [DOI: 10.1063/1.2214143]

The free-space electro-optical sampling (EOS) technique¹ is a powerful tool for measuring temporal structures of middle and far infrared electrical fields and frequency response of atoms, molecules, and materials.

An area of current interest is the application of EOS for noninterceptive, single-shot characterization of charged particle beams.^{2–5} One aspect in these experiments is the high-field amplitude. For example, for a bunch of 1 nC in 200 fs (a typical condition for the Linear Coherent Light Source⁶), the field 1 cm away from the electron beam is 3×10^7 V/m, while in a tabletop terahertz experiment the typical field strength is several orders of magnitude lower. In this case, distortions associated with the large dynamic range should be carefully examined.

There are several well known distortion effects in EOS measurement, such as the phase mismatch between the probe and the field under investigation,^{7,8} the bandwidth limit of the sampling crystal,⁹ and the beam propagation effect.¹⁰ In a recent paper, Jiang *et al.* have investigated the effect of operating at near-zero optical bias.¹¹ The scheme exploits the small residual birefringence in the sampling crystal as the optical bias in a crossed polarizer setup. From ellipsometry considerations,¹² the net signal is

$$I_s = I_0 [\cos \delta_0 - \cos(\delta + \delta_0)] \approx \frac{1}{2} I_0 \delta (\delta + 2\delta_0). \quad (1)$$

Here I_0 is the probe laser intensity, δ_0 and δ are, respectively, the phase retardation of the optical bias and that induced by the field under investigation. When $\delta_0 \gg \delta$, I_s is linear to δ . Jiang *et al.*¹¹ have examined the distortion when the quadratic term becomes important. In this letter, we extend the analysis for applications such as in beam-characterization experiments where δ can have a dynamic range far exceeding δ_0 .

The schematic of the experiment is shown in Fig. 1. The 70 fs, 0.78 mJ output of a Ti:Sa laser system is split into a probe and a pump beam. The pump beam, with 90% of the laser pulse energy, drives a 3 mm ZnTe crystal with (001) cut as the terahertz emitter. The laser spot size is 8 mm. An off-axis parabola focuses the terahertz onto a 1 mm ZnTe (001) sampling crystal. A single-shot detection technique based on the cross correlation between the terahertz field and the probe laser pulse¹³ is adapted. This method and its variation¹⁴ have been used in recent beam-characterization

experiments.^{4,5} The sampling crystal is sandwiched between a pair of crossed polarizers with the probe beam imaged onto a charge-coupled device camera. The setup has an extinction ratio better than 10^6 , which is reduced to 3500 when the sampling crystal is introduced.

The reduction of the extinction ratio is attributed to the residual birefringence in the sampling crystal. Scatterings due to surface roughness and internal defects are found to be small. In this case, one can measure the residual birefringence based on the extinction ratio. Considering multiple reflection between the crystal boundaries, we have

$$I_s = I_0 (1 - R)^2 (1 - a) \sum_{n=1}^{\infty} [R(1 - a)]^{2(n-1)} \times [1 - \cos(2n - 1)\delta_0]. \quad (2)$$

Here R and a are, respectively, the reflection at the surface and absorption in the crystal for a 800 nm laser, measured at $R=0.27$ (corresponding to an index of refraction of $n=3.2$) and $a=0.2$. n is the number of round trips in the crystal. With an extinction ratio of $I_s/I_0=3500$, we have a residue phase retardation $\delta_0 \approx 0.03$. This serves as an upper limit of the optical bias.

Another pair of polarizers is placed in front of the emitter crystal (Fig. 1). The second of them is fixed after they are adjusted to maximize the laser throughput. This way, by rotating the first polarizer we can adjust the laser intensity while maintaining its polarization on the emitter crystal. Noting that the laser is initially linearly polarized, after the first polarizer it has a polarization at θ from the input and an intensity of $\propto \cos^2 \theta$ according to Malus's law. Here θ is the azimuthal angle of the first polarizer relative to the maximum transmission position. Applying Malus's law again for the second polarizer, we obtain the final laser intensity on the emitter crystal of $I_{\text{pump}} \propto \cos^4 \theta$. This gives the terahertz field amplitude as $E_{\text{THz}} \propto I_{\text{pump}}$ or $E_{\text{THz}} \propto \cos^4 \theta$ before reaching saturation,^{15,16} hence the phase retardation $\delta \propto \cos^4 \theta$. The two polarizers also serve to balance the dispersion in the pump and the probe beam paths.

In addition, the azimuthal angle of the emitter crystal can be adjusted to allow flipping the polarity of the terahertz field with minimum change in the amplitude and shape of the wave forms. This quasirotational symmetry^{17,18} has been measured in a separate experiment. The setup makes it possible to compare the measurement on otherwise identical

^{a)}Electronic mail: ylli@aps.anl.gov

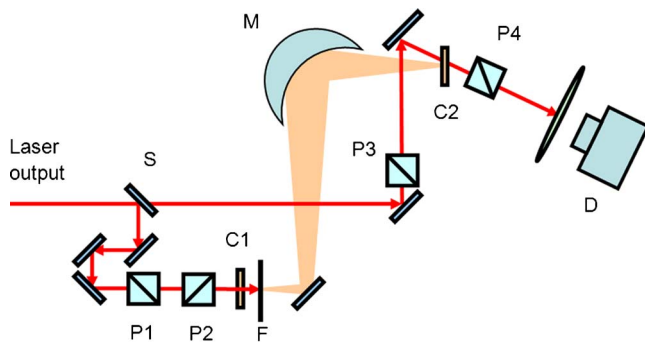


FIG. 1. (Color online) Schematic of the experiment. A Ti:Sa laser pulse is split by a beam splitter (S) into a pump and a probe beam. The pump beam generates the terahertz radiation on a 3 mm ZnTe crystal (C1) and is blocked by a 30 μm Teflon filter (F) after the crystal. The terahertz radiation is focused by an off-axis parabola (M) and crosses the probe beam on a 1 mm ZnTe sampling crystal (C2). A pair of cross polarizers (P3, P4) selects the modified probe which is imaged onto a charge-coupled device (CCD) camera (D) from the sampling crystal. The pump intensity on the emitter crystal is controlled by rotating polarizer 1 (P1) relative to polarizer P2. The polarity of the terahertz field can be flipped by rotating the emitter crystal (C1) azimuthally.

wave forms with opposite polarities at different amplitudes, free from any other potential distortions.

Figure 2 depicts two sets of wave form signals as a function of θ . In Fig. 2(a), the azimuthal angle of the emitter crystal and the laser control polarizers are optimized for the

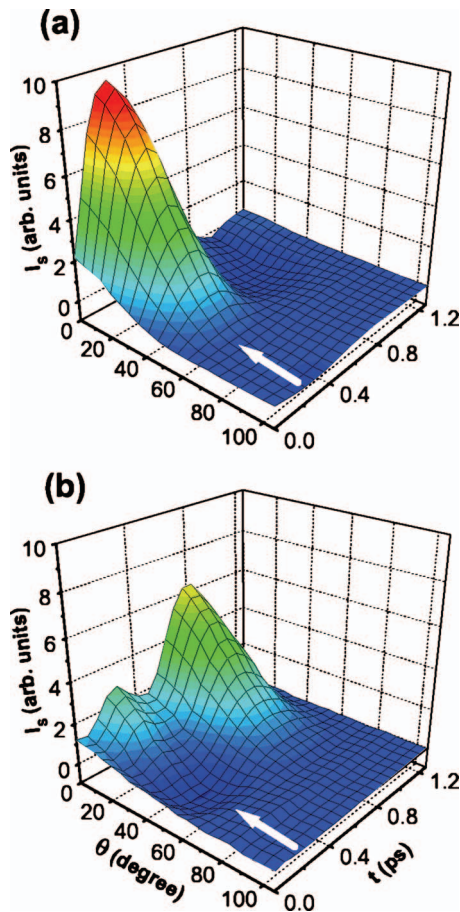


FIG. 2. (Color) Signal of single-shot terahertz waveforms as a function of the azimuthal angle of the first polarizer. The orientation of the 3 mm emitter ZnTe crystal was optimized for the signal at the indicated time in (a) and is rotated by 60° for (b).

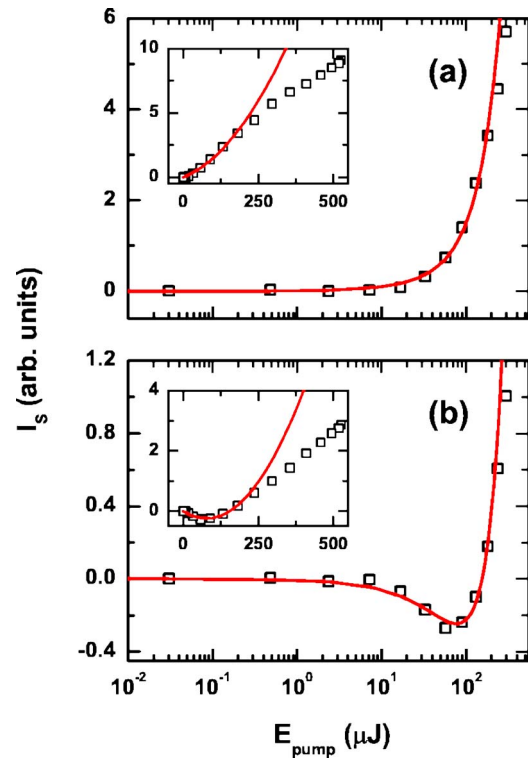


FIG. 3. (Color online) Signal as a function of the pump laser energy for the time indicated in Figs. 2(a) and 2(b). Symbols are the experimental data and curves are fittings using Eq. (1) assuming $\delta \propto I_{\text{pump}}$, which generates good agreement up to $E_{\text{pump}} = 200 \mu\text{J}$, beyond which the emitter crystal starts to saturate.

signal at the time slice indicated by the arrow. Figure 2(b) shows the wave form signals with the emitter crystal rotated azimuthally by 60° from those in Fig. 2(a). The two sets of wave forms underlining the signal in Figs. 2(a) and 2(b) are expected to be identical but with opposite polarities.

However, the wave form signals are more complicated than expected. In Fig. 2(a), the signal at the indicated time decreases monotonically from maximum to zero as the polarizer angle θ increases from 0 to 90°. The signal at the same time slice in Fig. 2(b), however, starts at a positive maximum, then decreases to a negative maximum at $\theta = 55^\circ$, then rises back to zero.

A more detailed analysis is given in Fig. 3, showing the signal at the indicated time slice as a function of the pump laser energy (after correcting for loss at the crystal entrance). At low pump laser intensities when $\delta \propto I_{\text{pump}}$, a fit using Eq. (1) gives excellent agreement to the data in Fig. 3(a) assuming δ has the same polarity as δ_0 . This quadratic dependence on pump energy, hence the terahertz field amplitude and the induced phase retardation, has been observed previously and can be corrected under certain conditions.^{4,11}

The signal in Fig. 3(b) shows a clear polarity change as the pump laser energy changes. However, this is just another result from Eq. (1) when δ_0 and δ have opposite signs. Fitting using Eq. (1) again generates excellent fit, with only δ_0 having a polarity opposite to that of δ . Obviously, for high-field applications, a signal at low level can easily be contaminated by this artificial signal polarity change that is not correlated to the field polarity. Without prior knowledge of the wave form, this distortion is impossible to correct.

At pump laser energies higher than 200 μJ , the experimental data deviate from the quadratic fit using Eq. (1) (Fig. 3(b)).

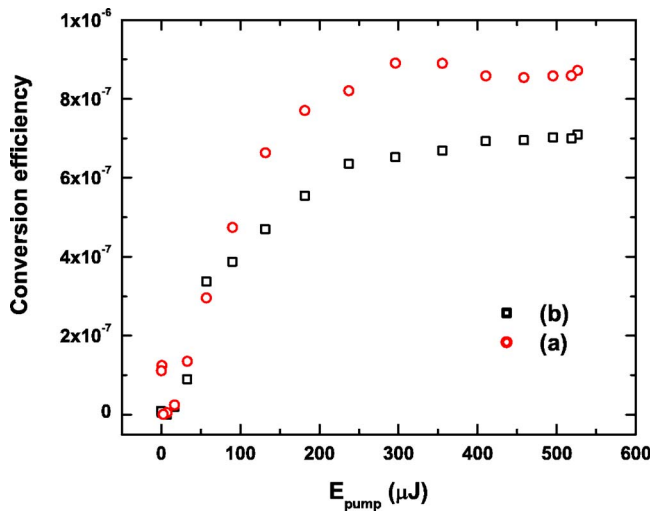


FIG. 4. (Color online) Conversion efficiency of the terahertz radiation as a function of the pump laser energy deduced from Figs. 3(a) (circles) and 3(b) (squares) using Eq. (1).

3, insets), which is due to the saturation in the terahertz emitter; thus the condition $\delta \propto I_{\text{pump}}$ no longer holds. The saturation is attributed to two-photon absorption of the pump beam and related free-carrier absorption in the ZnTe crystal¹⁵ and is studied in Ref. 16.

With the knowledge of δ_0 , the amplitude of the terahertz field can be estimated. From Eq. (1), $\delta = \delta_0$ at the negative signal maximum. Hence the field amplitude can be deduced through

$$\delta = \frac{2\pi\eta^3 E_{\text{THz}} l r_{41}}{\lambda} = 7.27 \times 10^{-4} E_{\text{THz}} l. \quad (3)$$

Here $\eta=3.2$ is the index of refraction, $r_{41}=4$ pm/V is the effective electrooptical coefficient, and $l=1$ mm is the thickness of the crystal. With $\delta=0.03$, we have $E_{\text{THz}}=8 \times 10^4$ V/m, taking into account the reflection loss at the exit of the emitter and the entrance of the sampling crystal. This corresponds to a power density of 8×10^6 W/m², with the focus size of 1.5 mm and a pulse duration of 2 ps; the energy per pulse is 30 pJ. At a pump energy of 57 μ J, the conversion efficiency to terahertz is 5×10^{-7} . In fact, the conversion efficiency as a function of the laser intensity is mapped out (Fig. 4), which gives a saturation conversion efficiency of 0.9×10^{-6} at 300 μ J of pump energy for the 3 mm ZnTe crystal in this experiment. A saturation conversion efficiency of 1.5×10^{-6} was obtained for a 2 mm ZnTe in Ref. 16.

In summary, we have measured the distortion of EOS signal at near zero optical bias. We identified the change of signal polarity due to the change in the terahertz field amplitude when the intrinsic optical bias has an opposite sign. This

was exploited to deduce the absolute field amplitude. This effect can distort signals in experiment with a large field dynamic range.

The authors thank K. Harklay, S. Milton, and K.-J. Kim for their support. This work is supported by the U.S. Department of Energy, Office of Science, Office of Basic Energy Sciences under Contract No. W-31-109-ENG-38.

¹Q. Wu and X.-C. Zhang, Appl. Phys. Lett. **67**, 3523 (1995); A. Nahata, D. H. Auston, T. F. Heinz, and C. Wu, *ibid.* **68**, 150 (1996); P. Uhd Jepsen, C. Winnewisser, M. Schall, V. Schyja, S. R. Keiding, and H. Helm, Phys. Rev. E **53**, R3052 (1996).

²X. Yan, A. M. MacLeod, W. A. Gillespie, G. M. H. Knippels, D. Oepts, A. F. G. van der Meer, and W. Seidel, Phys. Rev. Lett. **85**, 3404 (2000); I. Wilke, A. M. MacLeod, W. A. Gillespie, G. Berden, G. M. H. Knippels, and A. F. G. van der Meer, *ibid.* **88**, 124801 (2002).

³T. Tsang, V. Castillo, R. Larsen, D. M. Lazarus, D. Nikas, C. Ozben, Y. K. Semertzidis, T. Srinivasan-Rao, and L. Kowalski, J. Appl. Phys. **89**, 4921 (2001).

⁴G. Berden, S. P. Jamison, A. M. MacLeod, W. A. Gillespie, B. Redlich, and A. F. G. van der Meer, Phys. Rev. Lett. **93**, 114802 (2004).

⁵A. L. Cavalieri, D. M. Fritz, S. H. Lee, P. H. Bucksbaum, D. A. Reis, J. Rudati, D. M. Mills, P. H. Fuoss, G. B. Stephenson, C. C. Kao, D. P. Siddons, D. P. Lowney, A. G. MacPhee, D. Weinstein, R. W. Falcone, R. Pahl, J. Als-Nielsen, C. Blome, S. Düsterer, R. Ischebeck, H. Schlarb, H. Schulte-Schrepping, Th. Tschentscher, J. Schneider, O. Hignette, F. Sette, K. Sokolowski-Tinten, H. N. Chapman, R. W. Lee, T. N. Hansen, O. Synnergren, J. Larsson, S. Teichert, J. Sheppard, J. S. Wark, M. Bergh, C. Caleman, G. Hultdt, D. van der Spoel, N. Timneanu, J. Hajdu, R. A. Akre, E. Bong, P. Emma, P. Krejcik, J. Arthur, S. Brennan, K. J. Gaffney, A. M. Lindenberg, K. Luening, and J. B. Hastings, Phys. Rev. Lett. **94**, 114801 (2005).

⁶Linear Coherent Light Source Design Study Report No. SLAC-R-521, Stanford Linear Accelerator Center, 1998, <http://www-ssrl.slac.stanford.edu/lcls/cdr/>

⁷G. Gallot and D. Grischkowsky, J. Opt. Soc. Am. B **16**, 1204 (1999).

⁸H. J. Bakker, G. C. Cho, H. Kurz, Q. Wu, and X.-C. Zhang, J. Opt. Soc. Am. B **15**, 1795 (1998).

⁹A. Leitenstorfer, S. Hunsche, J. Shah, M. C. Nuss, and W. H. Knox, Appl. Phys. Lett. **74**, 1516 (1999).

¹⁰T. Hattori, R. Rungsaewang, K. Ohta, and K. Tukamoto, Jpn. J. Appl. Phys., Part 1 **41**, 5198 (2002).

¹¹Z. Jiang, F. G. Sun, Q. Chen, and X.-C. Zhang, Appl. Phys. Lett. **74**, 1191 (1999).

¹²J. Shan, A. S. Welington, E. Knoesel, M. Bonn, G. A. Reider, L. Bartels, and T. F. Heinz, Opt. Lett. **25**, 426 (2000).

¹³S. Jamison, J. Sehn, A. M. MacLeod, W. A. Gillespie, and D. A. Jaroszynski, Opt. Lett. **28**, 1710 (2003).

¹⁴M. Born and E. Wolf, *Principle of Optics*, 7th ed. (Cambridge University Press, New York, 2000), p. 24.

¹⁵F. G. Sun, W. Ji, and X.-C. Zhang, *Conference on Lasers and Electro-Optics* (Optical Society of America, Washington, D.C., 2000), pp. 479–480; *Lasers and Electro-Optics* (Optical Society of America, Washington DC, 2000), pp. 479–480.

¹⁶T. Löffler, T. Hahn, M. Thomson, F. Jacob, and H. G. Roskos, Opt. Express **13**, 5354 (2005).

¹⁷X. C. Zhang, Y. Jin, and X. F. Ma, Appl. Phys. Lett. **61**, 2764 (1992).

¹⁸P. C. M. Planken, H. K. Nienhuys, H. J. Bakker, and T. Wenckebach, J. Opt. Soc. Am. B **18**, 313 (2001).